Comparison of the physical, chemical and electrochemical properties of rayon- and polyacrylonitrile-based graphite felt electrodes

S. Zhong, C. Padeste, M. Kazacos and M. Skyllas-Kazacos*
School of Chemical Engineering and Industrial Chemistry, University of New South Wales, P.O. Box 1, Kensington, NSW 2033 (Australia)

(Received August 21, 1992; accepted November 25, 1992)

Abstract

Two typical graphite felts, based on rayon or polyacrylonitrile (PAN) precursors, are used as electrode materials for the vanadium-redox flow battery. The electrical resistivity, pore size and surface area of these felts are reported. The surface microstructure of the two felts is compared by using scanning electron microscopic SEM techniques. The differences in carbon–oxygen interaction behaviour between the two felts is investigated with X-ray photoelectron spectroscopic (XPS) techniques. The performance of vanadium-redox flow cells that employ either an untreated or thermally-treated graphite felt electrode is also evaluated. It is found that the electrical conductivity of the PAN-based felt is superior to that of its rayon-based counterpart. Although both felts have similar construction, the values of specific surface area are different. A difference in the surface microstructure is observed for the fibres from the two felts. XPS analysis reveals that the rayon-based felt reacts more easily with oxygen and forms C=O carbon–oxygen groups, while the PAN-based felt is more resistance to oxidation and preferentially forms C–O groups. It is believed that the more extensive oxygen interaction in the rayon felt is due to its microcrystalline structure.

Introduction

By virtue of their inertness to most chemicals and solvents, as well as their reasonable cost, carbon or graphite felts are widely used as electrode-active layers on carbon–plastic composite electrodes for redox flow-cell applications [1–7]. There are several hundred grades of carbon/graphite felts available from different sources. Researchers have found [5–7] that the variation in electrochemical activity from felt to felt is considerable. From the experimental results obtained, the electrical and electrochemical properties of graphite felts employed for application in the vanadium-redox flow cell are, indeed, quite different [8]. It has also been observed in our laboratory that some felts can be easily activated for vanadium redox reactions by a variety of oxidation methods [9], while others remain unaffected. Understanding the reasons for this behaviour will assist either the selection of a more suitable felt as the electrode-active layer, or the choice of an effective activation method for a particular type of felt. This, in turn, will further increase the efficiency and power density of the vanadium-redox flow battery.

*Author to whom correspondence should be addressed.

0378-7753/93/$6.00

In the present study, an evaluation and a comparison were made of two typical types of graphite felts (FMI and GFD 2, based on rayon and polyacrylonitrile, PAN, respectively) that are currently used as electrode materials for the vanadium-redox flow battery. First, the electrochemical activity of the two felt electrodes in the cell was determined in terms of cell resistance and cell efficiencies. The effect of thermal treatment on the electroactivity of the felt electrodes was then studied. The electrical conductivity, pore size and specific surface area of the two felts were compared. The surface microstructure of fibres from the two felts was examined by scanning electron microscopy (SEM). Finally, the two felts were thermally treated in either air or nitrogen gas, and the surface chemical properties of the fibres (such as surface composition and carbon–oxygen surface groups), were investigated with X-ray photoelectron spectroscopy (XPS).

Experimental

Graphite felt materials

The following felts samples were employed for this study: (i) (FMI: 3 mm thick, FMI graphite felt (Fibre Materials, Inc., Maine, USA), and (ii) GFD 2: 2.5 mm thick, (Sigri Electrographit GmbH, Germany).

Cell-resistance measurements and cell performance test

The electrochemical properties of the two graphite felt electrodes were evaluated in terms of cell resistance and cell efficiencies. FMI and GFD 2 graphite felts were used as electrodes for both halves of a vanadium-redox flow cell, the design of which has been described previously [9]. A piece of selemion CMV membrane (Asahi Glass Co., Japan) was employed as the separator. For cell resistance measurement, 50% state-of-charge (SOC) vanadium-redox electrolytes were employed, while for cell-performance testing, balanced vanadium-redox electrolytes were utilized [8]. The latter consisted of 2 M V(V) in 4 M H_2SO_4 and 2 M V(II) in 3 M H_2SO_4 for the positive and negative half-cells, respectively.

Electrical conductivity

The electrical conductivity of the different felt samples was determined by means of the ASTM D-991 method.

Surface area and pore size

The mercury-intrusion method was applied for measurement of the pore size and surface area of the different felts. An AutoPoro-9200 instrument (Micromeritics, USA) was employed, and the results were analysed and printed out by a computer system (Malvern Instruments, UK).

Thermal treatment of graphite felts

Samples of both FMI and GFD 2 graphite felts were placed in a furnace and heated up to 400 °C. After exposure to air at this temperature for 30 h, the samples were removed from the furnace, cooled down and stored in a sealed desiccator for surface analysis and for use as electrodes in the vanadium-redox flow cell. For comparison, another two samples were treated with nitrogen gas at the same temperature and for the same period.

SEM and XPS analysis

To compare the surface microstructure of the selected samples, the FMI and GFD 2 graphite felts were examined by SEM. The surface-chemical composition of the fibres, as well as the effect of thermal treatment on the surface characteristics of the two graphite felts, was analysed with XPS.

The SEM analysis was conducted with a S 360 scanning electron microscope unit (Laica Cambridge Ltd., UK).

The XPS spectra were recorded on a KRATOS XSAM AXIS 800 pci spectrometer equipped with a hemispherical analyser. Mg Kα radiation was used at a maximum power of 180 W. The base pressure in the analyser chamber was less than 10^{-9} torr (10^{-4} Pa). From each sample of felt, a piece of about 4 mm$\times$2 mm$\times$10 mm was cut and mounted on a stainless-steel sample holder. The analyser was run in the fixed transmission mode at a pass energy of 80 eV for wide-scan spectra and a pass energy of 40 eV for high-resolution spectra of the C1s and O1s regions. The spectrometer was calibrated on the Cu $2p_{3/2}$ line (E_B=932.7 eV) and the Ag $3d_{5/2}$ line (E_B=386.2 eV). Instrument control, as well as data collection and processing, was performed using KRATOS DS800 software on a PDP 11 computer.

Results and discussion

Electrochemical activity

The electrochemical activity of the two graphite felts (FMI and GFD 2) was evaluated and compared in terms of cell resistance and cell efficiencies when used as electrode materials for the vanadium-redox flow battery. The effect of thermal treatment on the electroactivity of the GFD 2 felt was also tested and compared with the results obtained in a previous study [9] with the FMI felt. The results are summarized in Table 1.

It can be seen from the data listed in Table 1 that for the untreated electrodes, relatively high cell resistance and corresponding low voltage efficiencies are obtained for both felts at a charge/discharge current density of 40 mA cm^{-2}. Thus, the polarization losses associated with the unactivated electrode materials are high. A lower cell resistance and higher cell efficiencies are observed, however, for the cell with GFD 2 felt electrode compared with that using FMI felt; this indicates that the former has better cell performance than the latter before treatment. A significant enhancement in cell performance is observed for both felt electrodes after thermal treatment: the

TABLE 1

Cell resistance and cell efficiency[a] of FMI [9] and GFD 2 graphite-felt electrodes in a vanadium-redox cell (CMV membrane, electrode area = 25 cm^2)

Electrode		Cell resistance R (Ω cm^2)	Cell efficiency at 40 mA cm^{-2} (%)		
			Coulombic	Voltage	Energy
Untreated on both sides	FMI	4.16	96.0	77.3	74.2
	GFD 2	3.03	94.0	80.9	76.2
Both sides thermally treated	FMI	2.34	98.2	87.2	86.0
	GFD 2	2.22	94.0	89.3	83.9

[a]Values are average of 10 charge/discharge cycles.

cell resistance values decreased and the cell voltage efficiencies increased greatly. A comparison of the cell resistance values for the two felts before and after treatment indicates, however, that the improvement in electrochemical activity after thermal treatment is slightly more pronounced for the FMI felt than for the GFD 2 felt. The differences in cell performance with the untreated felt electrodes, as well as the response towards thermal treatment of the two felts, suggest that the physical and chemical properties of the felt samples differ one from the other. Therefore, further investigations were conducted in an attempt to gain a better understanding of the relationship between the electrochemical behaviour and the physical and chemical characteristics of the two graphite felts.

Electrical resistivity

Table 2 gives the resistivity of untreated FMI and GFD 2 graphite-felt samples. Thermal treatment promotes no detectable change in the electrical resistivity for the two felts and, therefore, the data are not presented here. The results obtained again show the considerable difference between the two felts, i.e., the resistivity of FMI graphite felt is much higher than that of the GFD 2 variety. The differences in electrical resistivity of the two felts could be due to surface characteristics that are determined by the precursors and manufacturing factors, since the raw materials used and the processing procedure employed would affect the microstructure of the fibre [10–13]. Three types of precursors are most commonly used for graphite fibre and felt manufacture: rayon, PAN and pitch [10]. As reported by the manufacturers, the precursor for GFD 2 felt is PAN, while FMI felt is based on rayon. The significant difference in electrical resistivity between these two types of felt samples is thus probably associated with the different precursors used in their manufacture. It is also likely that the difference in resistivity of the two felts is caused by differences in the processing procedure that determines the graphitization stage of the felt materials [11]. Due to limited information from the manufacturer, however, it is not possible to discuss this further. The resistivity results are consistent with the measured values of cell resistance (Table 1), but this only partially explains the different cell performance behaviour of the two felts. The cell resistance consists of electrical resistance from cell components, such as electrode materials and the membrane, together with the faradaic resistance of the electrode reactions (i.e., electrochemical activity). An electrode material with high electrical resistivity would thus lead to high ohmic losses and poor cell performance. The low resistivity of both graphite felts, however, can account for only a small fraction of the total cell resistance. Other factors must therefore be responsible for the observed results.

Surface area and pore size

Figure 1 shows typical surface-area curves and illustrates the structural characteristics of the GFD 2 graphite felt. The cumulative curve in Fig. 1(a) levels off when the

TABLE 2

Comparison of electrical resistivity of FMI and GFD 2 graphite felts

Felt	Precursor	$\Delta V/I$ (Ω)	Thickness (mm)	Resistivity (Ω cm)
FMI	Rayon	0.100	3	0.023
GFD 2	PAN	0.038	2.5	0.0038

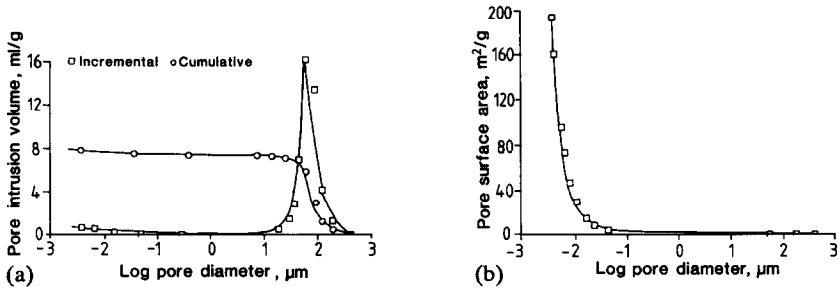

Fig. 1.Pore and surface-area distribution of GFD 2 graphite felt: (a) pore intrusion volume, and (b) cumulative surface area.

TABLE 3

Surface characteristics comparison of FMI and GFD 2 graphite felts

Felt	Thickness (mm)	Main pore diameter (μm)	Main pore volume/total measured pore volume (%)	Specific surface area for main pores ($m^2\ g^{-1}$)	Specific surface area for total measured pores ($m^2\ g^{-1}$)
FMI	3	188.5–36.5	93.2	0.329	238.27
GFD 2	2.5	188.5–13.0	92.8	0.390	266.86

pore diameter is smaller than 10 μm, while the incremental curve shows a dramatic increase in pore volume in the pore diameter range 10 to 100 μm. This indicates that the pore volume of the felt is attributed principally to the macropores, or more precisely, to the spaces between the fibres of the felt. This type of pore is commonly defined as the 'main pore' [14]. Figure 1(b) shows the cumulative surface area as a function of pore diameter. It can be seen that the high surface area of the felt is mainly attributed to the micropores that are about 0.01 to 0.001 μm in diameter. The structural properties of the FMI felt were also tested with the same techniques and similar properties were observed. The total measure specific surface area and pore-volume values of the two felts are listed in Table 3.

The main pore diameter for the two felt samples is between 10 and 100 μm, and the main pore volume is more than 90% of the total measured pore volume. These values indicate that the structure of the felt samples is similar. Nevertheless, differences in surface area are observed, and thus there is a difference in the microstructures of the two felt samples. The specific-surface area of the GFD 2 felt is slightly greater than that of the FMI felt, and this may partly account for the lower electrical resistivity (i.e., due to a higher contact area during resistivity measurements). A significant difference in specific surface area between main pores and total measured pores for each felt sample is also noted; this illustrates the unique structural characteristics of the graphite felts, i.e., the coexistence of macropores (space between fibres of the felt) and micropores. This phenomenon has been reported by Ashimura and Miyake [14].

The values of the main pore volume and the specific surface area are of most concern in battery applications. This is based on the following consideration. During battery operation, the bulk electrolyte cannot flow into the tiny pores of the felt so

that the electroactive species will become depleted within the pores and concentration polarization will be promoted. Since these tiny pores will not contribute to the effective electrode area, only the surface area for the main pores should be considered for electrochemical purposes. A similar treatment of the measured data can be found in ref. 14. The higher specific surface area for the main pores of the GFD 2 felt would again explain the observed lower cell-resistance values due to reduced polarization losses during charge/discharge in the vanadium-redox cell.

Surface microstructure of fibres in FMI and GFD 2 felts

The morphology of fibres from the FMI and GFD 2 felts was examined by SEM and is shown in Figs. 2 and 3, respectively. Since thermal treatment of the felt samples does not cause any visible change in the morphology of the fibres, micrographs for the treated samples are not given here. The individual fibres from the two felts have a totally different appearance. The fibres from the FMI felt (Fig. 2(a)) have an uneven and dusty surface, while GFD 2 fibres have a clean and smooth surface (Fig. 2(b)). Figures 3(a) and 3(b) provide a comparison of the cross sections of the FMI and GFD 2 fibres, respectively. It is clear that the structure of individual GFD 2 fibres is uniform and solid, while in the case of the FMI sample, the individual fibres appear to be bundles of several fibres. When the structural characteristics of the graphite-felt fibres give rise to edge planes and a high defect concentration [11], it would be expected that the fibres would react with oxygen and form highly oxidized carbon–oxygen groups more readily [10–13]. Further investigations of the two graphite felts were thus carried out with the XPS techniques and the results are presented below.

Surface chemical properties of fibres in FMI and GFD 2 graphite felts

As reported by Golden *et al.* [11], and supported by experimental results obtained previously in this laboratory [9], graphite-felt electrodes can be activated by thermal treatment in air. The latter causes a slight oxidation of the surface. Treatment for 30 h at 400 °C was found to give the best results. The effect of such thermal treatment on the FMI and GFD 2 fibres was analysed with XPS. The results are shown in Figs. 4 to 7 and are summarized in Table 4.

Surface composition

Figure 4 shows a typical example of an XPS wide-scan spectrum of a FMI felt sample. In all samples, only signals of carbon and oxygen were detected. This indicated that the content of other elements (except hydrogen) is very low.

The surface oxygen content of the samples, before and after different treatments, was determined from the XPS peak areas after subtraction of a linear background (Table 4). The results indicate that both of the untreated FMI and GFD 2 fibres are contaminated with volatile C–O compounds that are removed by treatment in N_2 at 400 °C. Thereafter, the surface concentration of oxygen is very low for both samples, and especially for the GFD 2 felt. Compared with the untreated sample, the oxygen content of the GFD 2 samples decreases after treatment in either N_2 or air, while for the FMI, a slight increase is observed for samples treated in air and a decrease for samples treated in N_2. Comparing the oxygen content of same type of felt subjected to different treatments, it can be seen that for the GFD 2 samples, treatment in air leads to a slightly higher oxygen concentration than in N_2, while for the FMI samples, this effect is more pronounced. These results indicate that the two felts have a different ability to interact with oxygen. The FMI felts react readily with oxygen and this suggests more edge planes and a less 'graphitic' surface structure [12] compared with the GFD 2 felt (Figs. 2 and 3).

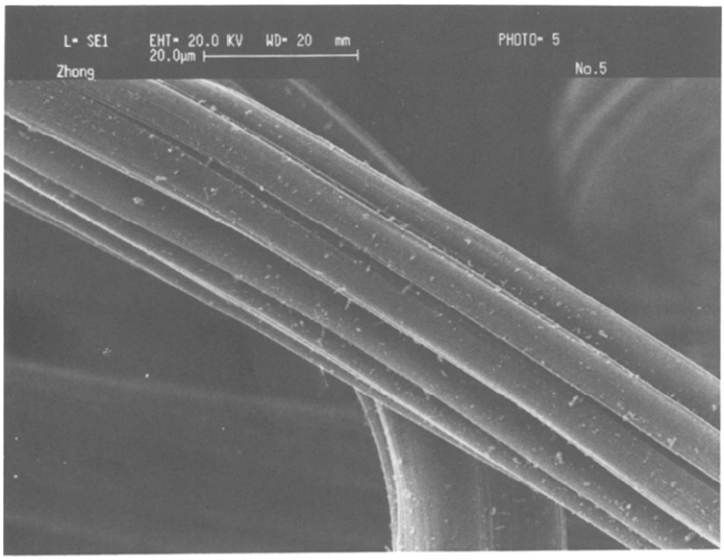

(a)

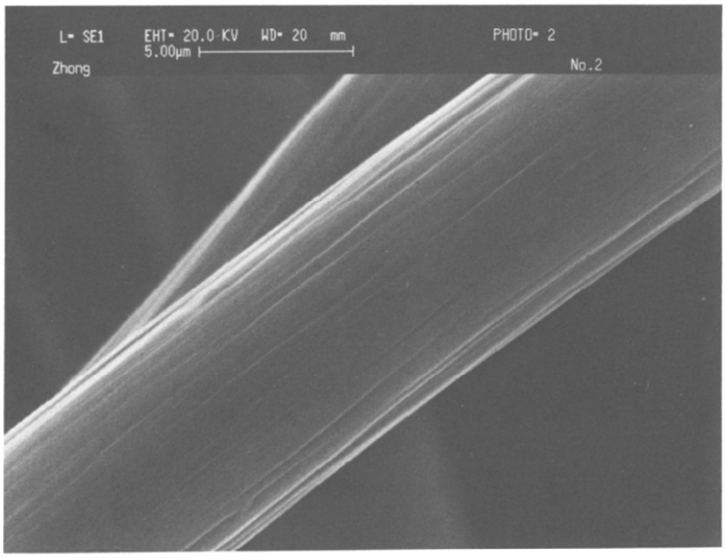

(b)

Fig. 2. Side-view of graphite felt fibres: (a) FMI, and (b) GFD 2.

The above results relate only to the total surface-oxygen content of the graphite-felt samples. For further information of the differences in electrochemical activity of the felts, more detailed analysis of the XPS spectra was undertaken, as described below.

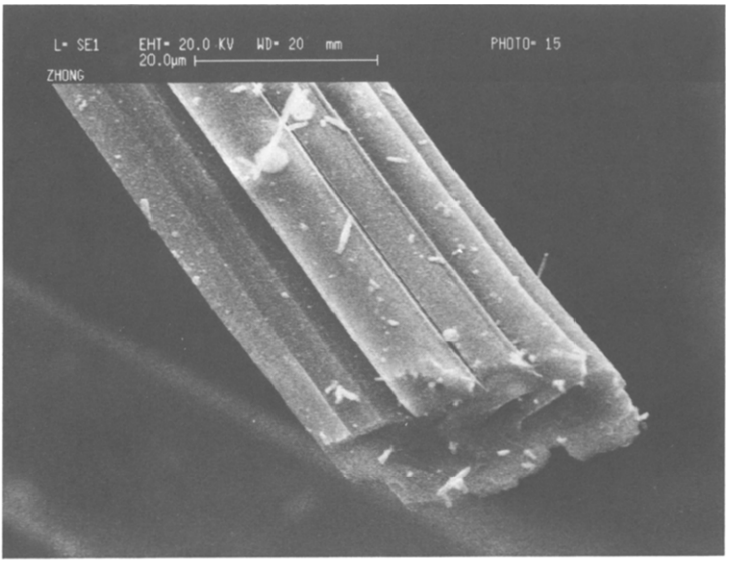

(a)

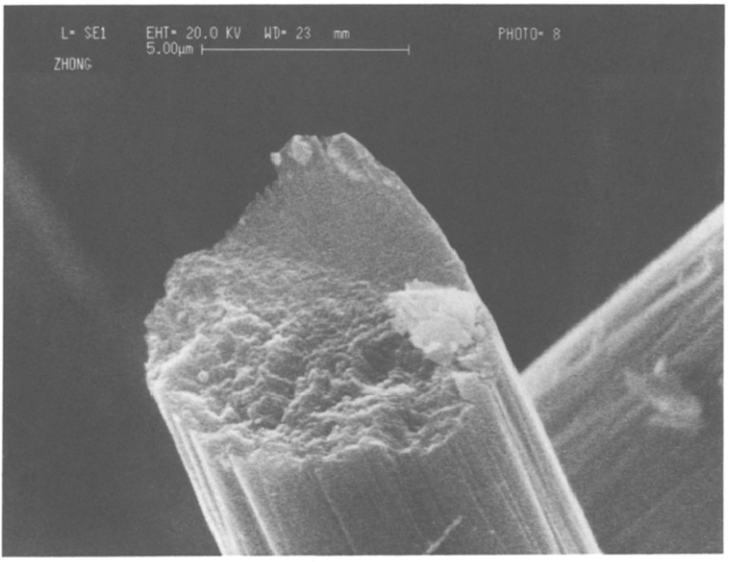

(b)

Fig. 3. Cross section of graphite felt fibres: (a) FMI, and (b) GFD 2.

Surface carbon–oxygen functional groups

Figure 5 shows the C1s region spectra for the FMI and GFD 2 felt samples treated in N_2 and air environments. The basic shape is asymmetric with a tailing at the high binding energy side that is typical for highly graphitized carbon fibres [15]. The treatment in air leads in both cases to a slightly increased relative intensity at the high binding energy side of the main peak; this indicates the formation of

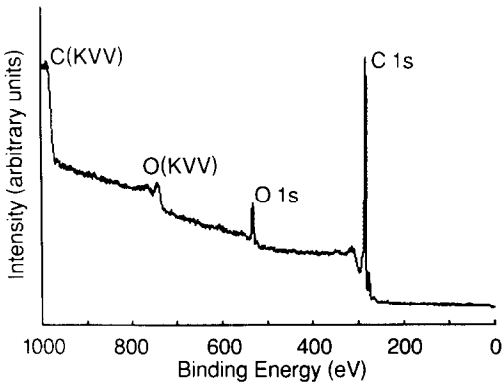

Fig. 4. Overall XPS spectra of FMI graphite-felt fibres treated in air at 400 °C for 30 h.

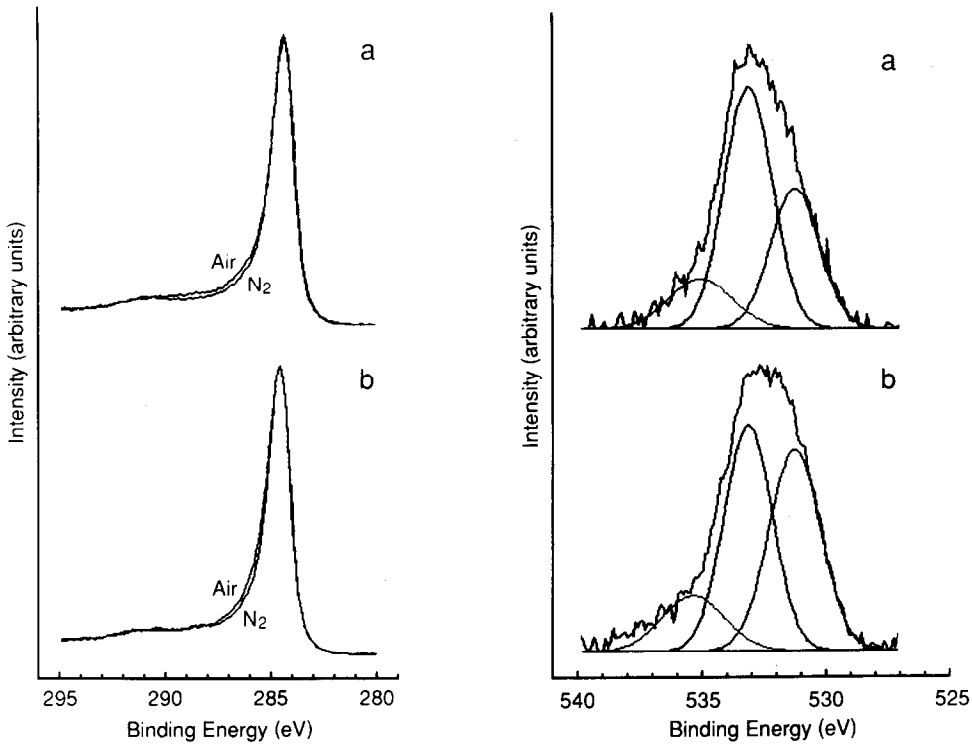

Fig. 5. C1s region XPS spectra of graphite-felt fibres treated in air and in N_2 at 400 °C for 30 h: (a) FMI, and (b) GFD 2.

Fig. 6. Fitted O1s XPS spectra of FMI graphite-felt fibres treated at 400 °C for 30 h: (a) in N_2, and (b) in air.

carbon–oxygen species. The differences in these spectra are not sufficiently pronounced to permit a more detailed analysis of the surface functional groups. As a consequence, curve fitting had to be performed on the corresponding O1s spectra, that display

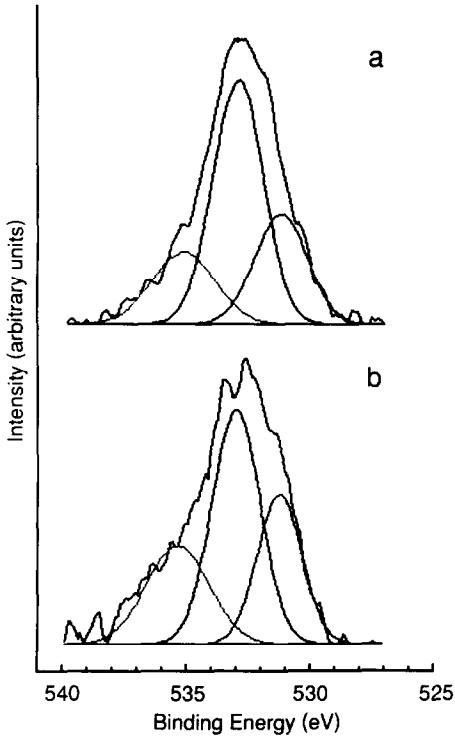

Fig. 7. Fitted O1s XPS spectra of GFD 2 graphite-felt fibres treated at 400 °C for 30 h: (a) in N_2, and (b) in air.

relatively poor signal-to-noise ratios due to the low amount of oxygen present in the samples.

Figures 6 and 7 illustrate the curve fitting of the O1s spectra for the FMI and GFD 2 felt samples after different treatments. All measured spectra could be fitted by three peaks: peak 1 (~535.5 eV) has the lowest intensity in all cases, and is due to the adsorbed water and probably some chemisorbed oxygen [16]; peak 2 (~533.0 eV) and peak 3 (~531.1 eV) are the O1s signals from C–OH and C=O (or/and C–O–C) functional groups, respectively [16]. The effect of the different treatments on the binding energy and the area ratio of each peak for the two felts is also summarized in Table 4. In the case of the untreated felt samples, only the total surface-oxygen content was determined. No attempt was made to further analyse the XPS spectra since surface contamination of the felt gave rise to considerable interference in the signal. It can be seen that for the GFD 2 sample (Fig. 7), treatment in air results in a slightly higher C–OH surface groups compared with the N_2-treated sample. For the FMI felt (Fig. 6), air treatment causes a considerable increase in the C=O surface groups that is accompanied by a decrease in C–OH surface concentration. These results suggest that the FMI felt has a strong tendency to interact with oxygen and prefers to form highly oxidized C=O species.

Thus, although the two felts studied here show a different tendency for surface-oxygen group formation, both felt types exhibited significant improvement in electrochemical activity after thermal treatment. The reason for this is still not well understood.

TABLE 4

XPS data for FMI and GFD 2 graphite felts

Characteristics	GFD			FMI		
	Untreated	N_2, 400 °C, 30 h	Air, 400 °C, 30 h	Untreated	N_2, 400 °C, 30 h	Air, 400 °C, 30 h
Atomic concentration of oxygen (%)	10.4	2.9	3.6	8.6	5.7	10.1
C1s peak, b.e.,[a] (eV)	[b]	284.6	284.6	[b]	284.6	284.6
O1s peak 1, b.e., (eV) (area, %)		535.6(21)	535.6 (13)		535.4 (10)	534.9 (11)
O1s peak 2, b.e., (eV) (area, %)		533.0 (52)	533.0 (62)		533.0 (56)	533.0 (41)
O1s peak 3, b.e., (eV) (area, %)		531.1 927)	531.2 (25)		531.1 (34)	531.2 (48)
C=O/C–O area ratio		0.53	0.40		0.61	1.18

[a]Binding energy (eV).

[b]Not determined due to interference from surface contamination.

A partial explanation could be the increase in wettability that is caused by burning off any greasy film formed on the surface of the fibres during processing. Other factors, such as residual impurities from the precursors or processing steps, could also have an important effect on the electrochemical properties of the graphite-felt electrodes, as well as on their susceptibility to oxidation.

Conclusions

Considerable differences in the characteristics of two graphite-felt materials from different sources have been observed. PAN-based graphite felt exhibits better electrical conductivity and electrochemical activity than the rayon-based counterpart selected for this study. The microstructure of fibres from the PAN-based felt is smooth and solid, while that from the rayon-based felt shows an uneven and bundle structure. The more extensive carbon–oxygen interaction of the latter suggests the presence of more edge planes and a higher surface-defect concentration. This causes the rayon-based felts to exhibit a higher surface-oxygen concentration and to form C=O groups more readily during thermal treatment compared with the PAN-based felt. While the role of different carbon–oxygen surface groups in determining the activity of the graphite-felt electrodes is still not fully understood, it is clear that a number of factors contribute to the electrochemical behaviour of these materials. Thus, in addition to surface functional groups, physical properties such as electrical conductivity, surface area, microstructure, hydrophilicity and precursor material must also be examined. It is likely that no one single property can be isolated to explain the differences in the electrochemical behaviour of different graphite-felt electrode materials.

Acknowledgement

This work was funded by a grant from the Australian Research Council.

References

1 M. Kazacos and M. Skyllas-Kazacos, *J. Electrochem. Soc., 136* (1989) 2759.
2 M. Skyllas-Kazacos, D. Kasherman, D. R. Hong and M. Kazacos, *Proc. Solar '89 Conf., Australia and New Zealand Solar Energy Society, Nov. 30–Dec. 2, 1989, Brisbane, Australia,* p. 40.
3 Redox flow cell development and demonstration project, *NASA TM-79067,* US Department of Energy, 1979, p. 31.
4 NASA redox storage system development project, Calendar Year 1980, *DOE/NASA/12726-18, NASA TM-82940,* 1982, p. 19.
5 K. Nozaki, H. Kaneko, A. Negishi and T. Ozawa, *Proc. Symp. Advances in Battery Materials and Processes, Washington, DC, USA, 1983,* Vol. 84-4, The Electrochemical Society, Pennington, NJ, 1984, p. 143.
6 K. Nozaki and T. Ozawa, *Proc. 17th Intersoc. Energy Conv. Eng. Conf., Los Angeles, CA, USA, Aug. 8–12, 1982,* p. 610.
7 K. Nozaki, O. Hamamoto, K. Mine and T. Ozawa, *Denki Kagaku, 55* (1987) 229.
8 S. Zhong, Carbon-plastic composite electrodes for the vanadium redox flow battery applications, *Ph.D. Thesis,* University of New South Wales, Australia, 1992.
9 B. Sun, The studies in electrode activation for vanadium redox flow battery applications, *Ph.D. Thesis,* University of New South Wales, Australia, 1991.

10 P. A. Thrower, *Proc. Workshop Electrochemistry of Carbon, Cleveland, OH, Aug. 1983,* Vol. 84-5, Proc. Vol. 84-5, The Electrochemical Society, Pennington, NJ, p. 40.
11 T. C. Golden, R. G. Jenkins, Y. Otake and A. W. Scaroni, *Proc. Workshop Electrochemistry of Carbon, Cleveland, OH, USA, Aug. 1983,* Proc. Vol. 84-5, The Electrochemical Society, Pennington, NJ, p. 61.
12 L. S. Singer, *Proc. Workshop Electrochemistry of Carbon, Cleveland, OH, USA, Aug. 1983,* Proc. Vol. 84-5, The Electrochemical Society, Pennington, NJ, p. 26.
13 L. S. Singer and I. C. Lewis, *Appl. Spectrosc., 36* (1982) 52.
14 S. Ashimura and Y. Miyake, *Denki Kagaku, 39* (1971) 944.
15 A. Proctor and P. M. A. Sherwood, *J. Electron Spectrosc. Relat. Phenon., 28* (1982) 39.
16 Y. Xie and P. M. A. Sherwood, *Chem. Mater., 1* (1989) 427.